Disease Models & Mechanisms 5, 389-396 (2012) doi:10.1242/dmm.008631

neb: a zebrafish model of nemaline myopathy due to *nebulin* mutation

William R. Telfer[1], Darcee D. Nelson[2], Trent Waugh[1], Susan V. Brooks[2,3] and James J. Dowling[1,4,*]

SUMMARY

Nemaline myopathy is one of the most common and severe non-dystrophic muscle diseases of childhood. Patients typically present in infancy with hypotonia, weakness, delayed motor development, and bulbar and respiratory difficulties. Mutations in six different genes are associated with nemaline myopathy, with nebulin mutations being the most common. No treatments or disease-modifying therapies have been identified for this disease. One of the major barriers to treatment development is the lack of models amenable to rapid and coordinated testing of potential therapeutic strategies. To overcome this barrier, we have characterized the first zebrafish model of nemaline myopathy. This model, termed *neb*, harbors a recessive mutation in the *nebulin* gene that results in decreased Nebulin protein levels, a severe motor phenotype and premature lethality. In addition to impaired motor function, *neb* zebrafish exhibit many of the features associated with human nemaline myopathy. These include impaired force generation, altered thin filament length and the presence of specific histopathological changes, including the formation of nemaline bodies. In summary, *neb* zebrafish mirror the genetic, clinical and pathological aspects of nemaline myopathy due to *NEB* mutation, and thus are an excellent model for future therapy development for this devastating disorder.

INTRODUCTION

Nemaline myopathy (NM) is one of the most common congenital muscle diseases, with an estimated prevalence as high as 1:20,000 in some populations (Darin and Tulinius, 2000). The typical clinical presentation is one of neonatal hypotonia, severe weakness, feeding intolerance and respiratory insufficiency, although there is clear variability in age of onset and clinical severity (Laing and Wallgren-Pettersson, 2009). A subset of infants with NM die in the first year of life, and the majority of others have significant morbidity and early mortality related to motor function impairment, feeding difficulties and respiratory failure (Ryan et al., 2001). The diagnosis of NM is established from muscle biopsy with the documentation of rod-shaped structures (called nemaline rods or bodies) by either light or electron microscopic examination (North and Ryan, 1993). Additional histopathological features include type I fiber predominance and atrophy.

To date, mutations in six genes, all associated with the actin thin filament portion of the contractile apparatus, have been reported in patients with NM (Laing and Wallgren-Pettersson, 2009). Recessive mutations in nebulin (*NEB*) and dominant or de novo mutations in *ACTA1* are the most common causes (Pelin et al., 1999; Sparrow et al., 2003; Lehtokari et al., 2006). The other genes mutated in NM are *TPM2* (Donner et al., 2002), *TPM3* (Laing et al., 1995), *CFL2* (Agrawal et al., 2007) and *TNNT1* (Jin et al., 2003), with mutations in all but *TPM3* being exceedingly rare (North and Ryan, 1993). The unifying pathomechanism in NM is thought to be reduced force generation as a result of impaired thin filament function (Ochala, 2008).

NEB is one of the largest genes in the human genome, with 183 exons encoding a 26,000 bp mRNA and a 600-900 kDa protein (Donner et al., 2004). The name nebulin is derived from 'nebulous', given because the function of the gene was obscure for many years (Ottenheijm and Granzier, 2010; Pappas et al., 2011). Recently, work from several laboratories has taken advantage of mouse knockout models and patient-derived myotubes to bring the function(s) of nebulin into focus. The major function of nebulin is to regulate the length of the thin filament (McElhinny et al., 2005; Bang et al., 2006; Witt et al., 2006; Chandra et al., 2009; Ottenheijm et al., 2009), a function it probably accomplishes by serving as a massive scaffold and ruler upon which actin filaments assemble. Loss of nebulin results in impaired thin filament length, changing it from 1.0-1.3 mm to 0.4-1.2 mm. Impaired thin filament length, in return, results in reduced contractile strength and diminished force generation.

As mentioned, nebulin knockout mice have been generated and characterized (Bang et al., 2006; Witt et al., 2006). These murine models recapitulate the salient features of human *NEB* mutation, including severe muscle weakness, impaired force generation and histopathological changes including reduced thin filament length and the presence of nemaline rods and bodies. Rodent models that recapitulate the features of NM additionally exist for *ACTA1* and *TPM3* (de Haan et al., 2002; Ravenscroft et al., 2011). Currently, no preclinical models have been characterized for *TPM2*, *CFL2* or *TNNT1*.

No treatments exist for NM, nor are there any candidate therapies under consideration. One of the significant barriers to therapy development is the lack of a model system amenable to rapid analysis of target therapeutics. Although excellent for studying pathomechanisms and for very targeted therapy development and testing, murine models are not amenable to larger scale testing of potential chemical modifiers of disease. Conversely, invertebrates

Departments of [1]Pediatrics, [2]Biomedical Engineering, [3]Molecular and Integrated Physiology, and [4]Neurology, University of Michigan Medical Center, Ann Arbor, MI 48109-2200, USA
*Author for correspondence (jamedowl@umich.edu)

Received 19 August 2011; Accepted 9 November 2011

such as *Drosophila* and *Caenorhabditis elegans* are not suitable for study of NM because they lack key components of the thin filament structure (such as, for example, nebulin). An ideal model system for the study of NM, particularly as it relates to drug development, is the zebrafish. Zebrafish contain all of the known NM genes, have a skeletal muscle structure highly similar to human skeletal muscle, and are amenable to large-scale chemical and genetic screens.

We have thus initiated the characterization of the first zebrafish model of NM. Utilizing an identified and publicly available mutant line (termed *neb*) in the *nebulin* gene generated by ENU mutagenesis at the Sanger Institute Zebrafish Mutant Resource, we have defined the behavioral, morphological, functional and histopathological features of the *neb* zebrafish. Our analysis revealed that *neb* zebrafish recapitulate all of the relevant features of NM due to nebulin mutation, and thus are an ideal model for future drug discovery for this severe and currently untreatable disorder.

RESULTS

neb zebrafish carry a *nebulin* mutation that alters RNA processing and protein levels

We obtained adult zebrafish heterozygous for a point mutation in the *neb* gene from the Sanger Institute Zebrafish Mutation Resource (allele hu2849; http://www.sanger.ac.uk/cgi-bin/Projects/D_rerio/zmp/gene.pl?id=ENSDARG00000032630). We verified the mutation in these fish as IVS43+1G>A (Fig. 1A), a mutation in the canonical splice donor site predicted to abolish splicing of exon 43 (ENSDART00000061293). Exon 43 is the equivalent of exon 78 in human *NEB*, an exon with previously reported mutations in NM patients (Lehtokari et al., 2006). We performed multiple independent crosses between heterozygous carrier fish, and obtained embryos with an obvious motor phenotype and abnormal morphological appearance (termed *neb* embryos; Fig. 1B) at the expected Mendelian frequency (38/132 or 28.7%). As expected, sequencing of genomic DNA from several affected embryos (n=8) demonstrated that they were all homozygous for the G>A mutation (Fig. 1A).

To determine the consequence of the G>A mutation on *nebulin* RNA processing, we analyzed RNA from *neb* embryos and compared it with control embryos. Reverse-transcriptase PCR (RT-PCR) from wild-type siblings using primers to exons 42-44 produced an intense band of the expected size, one band of slightly larger size and a smaller band of much lower intensity. Analysis of RNA from *neb* embryos, by contrast, revealed only a faint band of expected size, no band of larger size and a more prominent smaller band of the size predicted with loss of exon 43 (Fig. 1C). Sequencing of the PCR products confirmed that the smaller band lacked exon 43 sequence, indicating that the G>A mutation is associated with exon 43 skipping (data not shown). Given that a faint amount of the normal-sized RNA product is present in *neb* embryos, splicing at exon 43 is probably not completely abolished by the G>A mutation. The presence of small amounts of the smaller RNA product in controls is consistent with the fact that our control group includes embryos that are heterozygous for the *neb* mutation.

On the basis of analysis of the zebrafish *nebulin* sequence, the *nebulin* open reading frame is maintained with loss of exon 43. To better understand the effect of the G>A mutation on Nebulin protein expression, we performed western blot analysis using two anti-Nebulin antibodies. Western analysis using an antibody to the N-terminus of Nebulin of protein extracted from wild-type siblings produced a band of very high molecular weight (>500 kDa). Analysis of protein from *neb* embryos, by contrast, failed to produce even a truncated band (Fig. 1D). An identical result was produced using the NB2 monoclonal antibody generated from full-length Nebulin (data not shown). These results indicate that either no Nebulin protein, or else a truncated Nebulin missing the N-terminus, is produced in *neb* embryos. Unfortunately, antibodies specific to the Nebulin C-terminus did not produce bands in either wild-type or *neb* embryos, so we were unable to fully characterize the Nebulin protein in mutant embryos. Of note, we verified the integrity of the protein extracted from *neb* embryos by reprobing the blot with antibodies to GAPDH (Fig. 1D) and desmin (data not shown).

neb embryos have a severe motor phenotype and display premature lethality

To further characterize the *neb* phenotype, we examined motor function in developing embryos. *neb* zebrafish were morphologically and functionally indistinguishable from unaffected clutchmates during the first 48 hours post fertilization (hpf). This was confirmed by measuring spontaneous coiling, a stereotyped motor behavior that occurs between 20-28 hpf (Saint-Amant and Drapeau, 1998). Examination of coiling in clutches from several *neb* +/– intercrosses revealed no changes in any of the resulting offspring, approximately 25% of which should exhibit the *neb* phenotype (n=200 embryos examined).

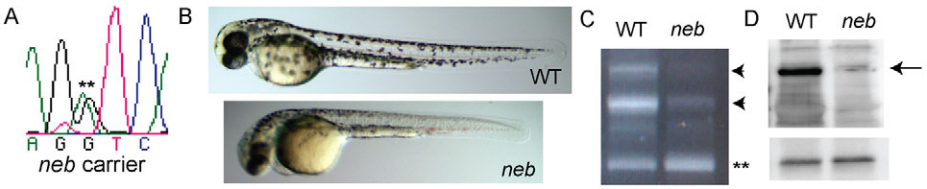

Fig. 1. Characterization of *neb* zebrafish. (A) DNA sequencing of *neb* adult carriers revealed a heterozygous sequence change (G>A) at IVS43+1 (**). (B) Live visualization of *neb* embryos and control (WT) littermates at 2 dpf. *neb* embryos are smaller and have thin bodies and tails. Genotyping confirmed that phenotypically abnormal embryos were homozygous for the G>A sequence change. (C) RT-PCR using exon 42-44 spanning primers of RNA extracted from pools of WT and *neb* embryos. WT fish have 2 major bands (arrowheads), a middle band that corresponds to the predicted size of exons 42-44 and a higher molecular weight band. *neb* zebrafish have diminished expression of these bands and instead have increased expression of a small band (**) with a size equal to that of exons 42-44 and excluding exon 43. Sequencing of this band confirmed that it lacked exon 43. (D) Western blot analysis of protein extracted from WT and *neb* embryos. Upper blot: with an anti-N-terminal Nebulin antibody, WT embryos had a single dominant band of very high molecular weight. This band was absent from *neb* embryos (arrow). Lower blot: confirmation of protein sample integrity and equal loading using anti-GAPDH antibody.

By 48 hpf, however, the *neb* phenotype was obviously apparent. The most notable observation was that affected embryos exhibited a paucity of movement. To better characterize this, we examined the touch-evoked escape response, a motor behavior that begins at approximately 48 hpf and that involves escape swimming in response to a mechanical stimulus. Wild-type embryos briskly swam away when touched on the tail with a metal probe (supplementary material Movie 1). Conversely, the best response to mechanical stimulation exhibited by *neb* embryos was tail quivering, and some embryos failed to display any movement (supplementary material Movie 2). We quantitated this observation using our previously developed 3-point scoring system for touch-evoked escape response (0=no movement, 1=tail contraction without swimming, 2=escape but movement of only 2-3 body lengths, and 3=normal escape) (Telfer et al., 2010). As measured at 72 hpf, a large and statistically significant difference was observed between *neb* mutants (n=20) and wild-type clutchmates (n=47; 1.0±0.1 vs 2.9±0.1, P<0.0001).

The *neb* phenotype continued to progress from 3 dpf onwards, with eventual elimination of all spontaneous and provoked movement and with markedly reduced survival. Larvae began dying at 5 dpf, and no *neb* mutants survived beyond 7 dpf (n=100). The abnormal morphological appearance of *neb* zebrafish also became progressively more apparent (Fig. 2A,B). In particular, *neb* zebrafish were smaller than wild-type siblings, had prominently bent tails, and developed pericardial and tail edema. Because edema can be due either to a lack of movement or to cardiac dysfunction, we examined the hearts of *neb* embryos and, although there was no striking morphological abnormalities in the hearts (Fig. 2A,B), heart rate was significantly slowed (supplementary material Movies 3, 4). Of note, *neb* larvae had abnormal muscle birefringence (Fig. 2C). Birefringence, an optical property of muscle when visualized using plane polarized light, is a measure of muscle integrity and is prominently reduced in zebrafish models of muscular dystrophy (Bassett and Currie, 2003). The changes in birefringence in *neb* zebrafish, although far less prominent than what is observed in models of muscular dystrophy (Fig. 2C), probably reflect disorganization of the underlying sarcomeric structure (see below).

neb larvae have impaired contractile properties

The inability of *neb* zebrafish to swim suggested a defect in muscle force generation. To define the contractile properties of *neb* larvae, we utilized a novel technique adapted from the study of rodent skeletal muscle. We elicited a single bilateral contraction of whole *neb* and wild-type larvae (n=5) and measured peak force and kinetics of force generation. Representative force responses from *neb* and wild-type larvae are shown in Fig. 3A. Peak forces generated by *neb* larvae were significantly less than forces generated by wild types (0.08±0.04 mN vs 0.46±0.04 mN, P<0.001). To ensure that the lower forces generated by *neb* larvae were not simply due to a smaller muscle, we normalized peak force generation to skeletal muscle cross-sectional area (CSA). *neb* larvae unsurprisingly had smaller muscle (0.018±0.001 mm^2 vs 0.023±0.001 mm^2, P<0.001); however, normalized peak force was still significantly lower in *neb* larvae than in controls (80% reduction as compared with controls; Fig. 3B). In contrast to the impaired force generation exhibited by *neb* larvae as compared with wild-type larvae, there were no significant differences in the kinetics of force generation between the groups, as determined by measuring time-to-peak force (TPF; in ms: 11.0±0.5 for *neb* vs 10.5±0.2 for wild type, P=0.383) and half-relaxation time (HRT; in ms: 10.6±1.7 for *neb* vs 8.5±0.2 for wild type, P=0.263).

neb skeletal muscle has altered thin filament length

One of the main functions of the nebulin protein is thought to be the establishment of the length of the thin filament; support for this idea comes from analysis of *Neb* knockout mice and from patient myotubes with *NEB* mutations (Bang et al., 2006; Witt et al., 2006; Gokhin et al., 2009; Ottenheijm et al., 2009). To examine thin filament length, we used both electron microscopic analysis and immunofluorescence studies. Electron microscopy was performed on 3-dpf control and *neb* zebrafish (Fig. 4A) (n=3 per condition). Skeletal muscle from control zebrafish displayed the expected appearance of the contractile apparatus, with easily distinguished Z-bands, thin filaments and thick filaments. By contrast, although still clearly present, these structures were less well delineated in *neb* skeletal muscle. In addition, both the total length of sarcomere (Fig. 4A, white arrow) and the length of the thin filament (Fig. 4A, red arrow) were quantitatively shorter than with controls (see below). This ultrastructural appearance is similar to that observed in *Neb* knockout mice (Bang et al., 2006; Witt et al., 2006) and in *NEB* patients (Ottenheijm et al., 2009).

To further study thin filament appearance, we used an immunohistochemical approach on myofibers isolated from control

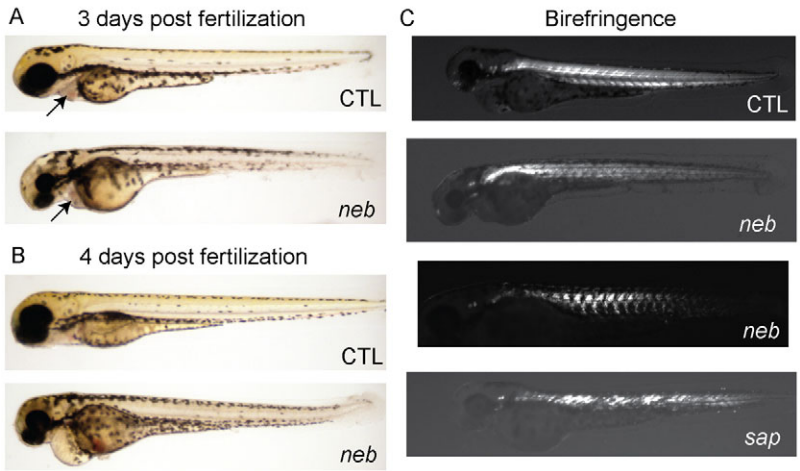

Fig. 2. *neb* embryos are morphologically abnormal and have disrupted birefringence. Live imaging of *neb* embryos and age-matched littermates (CTL) at 3 dpf (A) and 4 dpf (B). Compared with controls, *neb* zebrafish are smaller, have thin and bent tails, and have pericardial edema. The heart structure is not obviously abnormal (arrows and see supplementary material Movies 3, 4). (C) Live image analysis of 3 dpf embryos using polarized light to detect birefringence. Wild type (CTL) embryos have normal birefringence, whereas *neb* embryos have diminished and patchy birefringence. The pattern is variable between *neb* embryos. Depicted for comparison is an age-matched *sapje* (*sap*) embryo. *sap* zebrafish have a recessive mutation in dystrophin and abnormal birefringence.

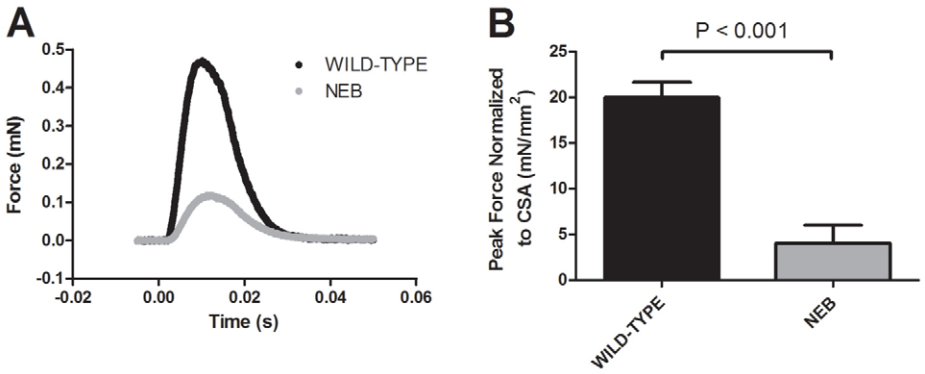

Fig. 3. Muscle contractions of *neb* larvae generate less force than wild-type larvae. Force generation was measured during a bilateral contraction of whole *neb* and wild-type larvae at 3 dpf (*n*=5). (A) Representative force response from *neb* and wild-type larvae. (B) Peak force normalized to cross-sectional area (CSA) was significantly less in *neb* larvae compared with wild type (4.0±2.0 mN/mm^2 vs 20±1.7 mN/mm^2, *P*<0.001). Data expressed as mean ± s.e.m.

and *neb* zebrafish. Isolated myofibers were co-immunostained with antibodies to α-actinin (Fig, 4B, red; marking the Z-band) and tropomodulin (Fig, 4B, green; marking the tip of the thin filament). Representative images from control and *neb* myofibers are presented in Fig. 4B.

Thin filament length was calculated both by measuring the distance from Z-line to H-zone using electron micrographs and by measuring the distance between red (α-actinin) and green (tropomodulin) signals from confocal immunofluorescent images. Quantitative comparison between groups revealed that *neb* thin filaments were reduced in length by nearly 30% (Fig. 4C and data not shown). These measurements are consistent with the observations from myofibers of NEB patients (Ottenheijm et al., 2009). Of note, it is apparent both with electron microscopic analysis and with immunostaining that some areas of the thin-filament–Z-band intersection are disorganized and/or poorly demarcated (arrow in Fig. 4B).

neb skeletal muscle contains nemaline bodies

The defining histological feature of human NM is the presence of nemaline bodies in the muscle biopsy. We thus examined the skeletal muscle of *neb* zebrafish for nemaline bodies by using both ultrastructural and immunohistological analyses. Using electron microscopy, we identified numerous areas containing abnormal clusters of sarcomeric material (Fig. 5A). Higher magnification of these regions revealed that these areas are mainly composed of filamentous material (Fig. 5A, bottom panel) and are thus reminiscent in appearance to nemaline bodies (Schroder et al., 2004). To further examine this, we used immunofluorescence on isolated myofibers with an antibody to α-actinin. As with electron microscopy, we saw numerous areas of accumulated α-actinin staining in *neb* myofibers (Fig. 5B). Co-staining with phalloidin (Fig. 5B, red) demonstrated that actin was also a component of these aggregates (Fig. 5B, bottom panel, arrow). Such accumulations of α-actinin have been reported in human NM myofibers (Wallgren-Pettersson et al., 1995) and, together with the electron microscopy observations, are consistent with the presence of nemaline bodies in *neb* zebrafish skeletal muscle. Of note, no such abnormalities were detected in the skeletal muscle of control zebrafish.

DISCUSSION

NM is a severe childhood-onset muscle disease without treatment or cure. Not only are there no current treatments for this condition, there are few viable therapeutic strategies in the research pipeline. The goal of the present study was to develop an in vivo reagent suitable for large-scale therapy development. In this vein, we have characterized a zebrafish mutant with all of the relevant features of NM. This mutant carries a recessive mutation in the *nebulin*

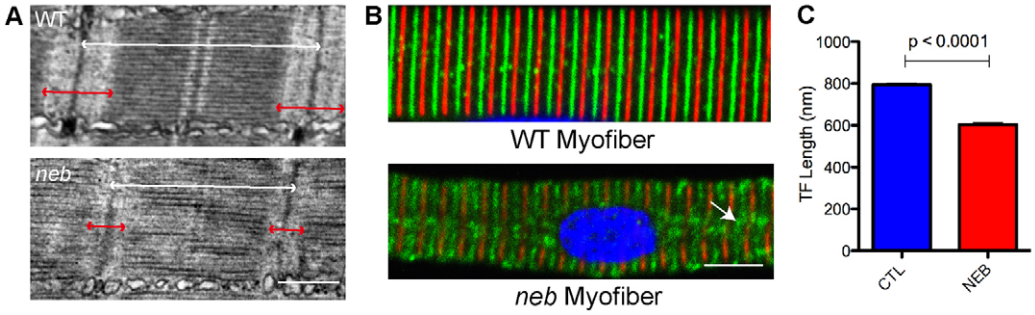

Fig. 4. Altered thin filament length in skeletal muscle from *neb* embryos. (A) Ultrastructural analysis of *neb* embryos and wild-type clutchmates at 3 dpf. Thin filaments (I bands; marked with red arrows) are qualitatively smaller in *neb* embryos compared with wild type. Overall sarcomere length is also reduced (white arrows). Scale bar: 500 nm. (B) Co-immunostaining of isolated myofibers with antibodies to α-actinin (red), to mark the Z-lines, and tropomodulin (green), to mark the ends of the thin filaments. Note that α-actinin staining is somewhat diminished in *neb* embryos and that there are areas of disorganization of tropomodulin staining (arrow). Scale bar: 10 µm. (C) Quantification of thin filament (TF) length. TF length was calculated using electron micrographs by measuring from the Z-line to the beginning of the H zone. TF length in *neb* zebrafish was significantly reduced (in nm) compared with controls (CTL): 794.3±5.7 vs 603.8±7.9, *n*=4 averaged measurements, *P*<0.0001.

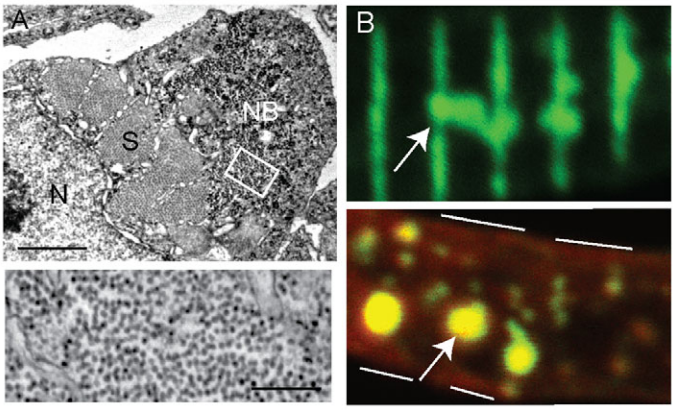

Fig. 5. Nemaline bodies in *neb* skeletal muscle. (A) Ultrastructural analysis reveals the presence of aggregates similar to nemaline bodies. Top panel: a typical example of a nemaline body (NB) is depicted in a myofiber examined in cross-section. S, sarcomere; N, nucleus. Scale bar: 1 µm. Bottom panel: higher magnification of the area denoted by the white box demonstrates that the aggregates are composed primarily of filamentous material. Scale bar: 250 nm. (B) Immunohistochemical analysis of isolated myofibers from 3-dpf *neb* embryos using an antibody to α-actinin. Top panel: frequent areas of aberrant α-actinin accumulation were detected (arrow), consistent with the presence of nemaline bodies. Bottom panel: co-staining with phalloidin (red) reveals the presence of actin in the aggregated areas (arrow). White lines denote the sarcolemmal membrane.

gene, and has impaired motor function, decreased survival, impaired force generation and the histopathological hallmarks of human NM.

neb as a model of human nemaline myopathy

As alluded to above, *neb* zebrafish share all necessary characteristics of human NM (Jones et al., 2003; Laing and Wallgren-Pettersson, 2009). They have a splice site mutation in the *nebulin* gene that causes missplicing and results in either a truncated or absent protein. Of relevance, Ottenheijm et al. recently examined nebulin protein expression in individuals with a *NEB* mutation similar to our zebrafish (exon 55 in-frame deletion), and found by western blot analysis that total nebulin levels were reduced approximately eightfold and that expression detected by using an N-terminal antibody was even more severely reduced (Ottenheijm et al., 2009). The more dramatic loss of the N-terminus was postulated to result from more selective degradation of the mutated or truncated N-terminus than of other aspects of the protein. On the basis of this study, we predict that overall Nebulin levels are dramatically reduced in *neb* zebrafish, but that there might be the presence of low abundance truncated Nebulin protein lacking the N-terminus. We were not able to test this prediction because additional anti-Nebulin antibodies did not show cross-reactivity with the zebrafish protein.

In terms of shared characteristics between *neb* zebrafish and both human *NEB* myofibers and the mouse knockouts, most striking are (1) the presence of nemaline bodies, (2) the reduction in thin filament length and (3) the reduction in force generation. Although nemaline bodies are not only seen in NM, they are the defining pathological characteristic of the disease. That we are able to detect them both by electron microscopy and by immunohistochemical analysis is in keeping with *neb* zebrafish as an excellent model of NM regardless of subtype. Reduction in thin filament length is more specific to *nebulin* mutation versus other genetic casues of NM. Previous studies have documented a mean difference in length of approximately 60% (McElhinny et al., 2005; Bang et al., 2006; Witt et al., 2006; Gokhin et al., 2009; Ottenheijm et al., 2009). In our study we describe a reduction to 70% of normal, which agrees well with the human data. Finally, we calculated mean force generation for *neb* mutants and found a severe reduction that is remarkably consistent with the values obtained with both *NEB* patient myofibers and from *Neb* knockout mice (Ottenheijm and Granzier, 2010; Labeit et al., 2011). This implies that *neb* zebrafish not only mirror the genetic and histological changes associated with *nebulin* mutation, but also model the most important skeletal muscle functional impairment as well. Of note, the measurement of contractile properties in the *neb* zebrafish demonstrates a novel technical approach for the study of zebrafish skeletal muscle function, and the fact that our data is so consistent with the previously reported data for *NEB* mutation indicates the validity and value of this novel experimentation.

One area in which *neb* zebrafish do differ from murine models and from individuals with *NEB* mutations is the fact that they seem to have a cardiac phenotype, as revealed by slowed heart rate and early onset of pericardial edema. No cardiac dysfunction has been reported in *Neb* knockout mice, although it has not been extensively examined and the mice die within 2 weeks of birth. In a large cohort study of NM patients, 6/143 individuals developed transient congestive heart failure at birth and only 2/143 had symptomatic heart disease outside of the neonatal period (Ryan et al., 2001). By contrast, 44% had abnormal electrocardiograms (ECGs; also known as EKGs), suggesting at least mild cardiac involvement.

The hypothesized explanation for the lack of cardiac involvement with *NEB* mutations is that a nebulin-like protein called nebulette is highly expressed in the heart and is believed to compensate for lack of nebulin function (Pappas et al., 2011). Given that a nebulette paralog is annotated in the zebrafish genome, the reason(s) for a more robust cardiac phenotype in *neb* zebrafish are as-yet unknown. One likely possibility is that zebrafish might be more dependent on nebulin for cardiac function than are mice or humans. Another is that the changes we observe in the zebrafish do not manifest as overt clinical symptoms in *NEB* patients. A final explanation is that the *neb* zebrafish line has a closely linked second site mutation in a gene important for cardiac function. Because we have outcrossed the *neb* mutation and, in addition, have never seen the cardiac phenotype in isolation, we feel that this is unlikely. However, it has not been conclusively excluded.

Utility of the novel *neb* zebrafish line

neb zebrafish, by sharing the cardinal features that define the human disease, are thus ideally suited for use for future therapy development for NM. In particular, given the unique advantages of the zebrafish system (large clutch sizes, rapid development and their ability to readily absorb small compounds), *neb* mutants will be particularly amenable to large-scale chemical screens with potential therapeutic agents. This is especially the case because *neb* zebrafish have easily screenable phenotypes, including severely impaired motor function (inability to swim) and greatly reduced

survival. In addition, *neb* zebrafish can serve as a value tool for testing gene-based therapies. For example, conventional gene therapy would be impossible for *nebulin* because of its large size. A potential approach would be the use of a truncated or mini-nebulin (Pappas et al., 2010), a strategy analogous to that employed for dystrophin gene replacement. Because of the ease of exogenous cDNA introduction and transgenic generation in zebrafish, *neb* zebrafish would be an excellent system for rapid in vivo testing of the suitability and efficacy of various mini-nebulin constructs.

neb zebrafish are also an ideal model system for further studies into disease pathogenesis. It is clear from this study and from the previous work in *Neb* knockout mice and *NEB* myofibers (Ottenheijm and Granzier, 2010; Labeit et al., 2011) that decreased force generation is a central aspect of the pathogenesis of *NEB*-associated NM. However, it is still uncertain what aspects of nebulin function are most important for force generation and thus it is not clear which function(s) need to be replaced in order to restore normal force in the absence of nebulin. For example, nebulin regulates thin filament length and also participates in the control of actin-myosin cross-bridge dynamics (Ochala et al., 2011; Ottenheijm et al., 2011). How each contributes to the overall generation of forceful contractions has yet to be determined. Future experimentation in the *neb* zebrafish, using, for example, *nebulin* rescue constructs defective in either thin filament length determination or else regulation of cross-bridge kinetics, will be instrumental in the resolution of these and other questions related to NM, especially given how well *neb* zebrafish recapitulate the force generation defects observed in patient myofibers.

In all, we have developed and characterized the first genetic model of NM in the zebrafish. This model will serve as an ideal platform for drug discovery experimentation as well as explorations into disease pathogenesis.

METHODS

Zebrafish husbandry

Zebrafish were housed, maintained and bred under UCUCA approved conditions. All experimentation and procedures were performed according to UCUCA approved specifications

neb zebrafish

neb zebrafish were obtained from the Sanger Institute zebrafish mutation project (line hu2849), and can be requested from the Zebrafish International Resource Center (ZIRC). *neb* zebrafish were initially outcrossed to AB line zebrafish (obtained from ZIRC).

Genotyping

Genomic DNA was extracted from tail fin biopsies (carriers) or whole embryos by proteinase K digestion followed by centrifugation and ethanol precipitation. Extracted DNA was subjected to PCR and then Sanger sequencing (performed by the DNA sequencing core at the University of Michigan).

RT-PCR

RNA was isolated from pools of embryos using an RNeasy Mini kit (Qiagen). Reverse transcription was performed using iScript reaction mix. PCR was accomplished using primers spanning exons 42-44. For sequencing, the relevant bands were gel extracted and then sequenced as above.

Western blot analysis

Protein was extracted from pools of embryos and then resolved on a 3-8% Tris-acetate gel (Invitrogen). Transfer was performed at 35V for 19 hours on ice. Bands were visualized using Amersham ECL plus (GE Biosciences). Anti-Nebulin antibodies were a kind gift of Carol Gregorio (University of Arizona, Tucson, AZ). Additional antibodies used were to desmin (Sigma) and GAPDH (Millipore). Secondary antibodies were obtained from Santa Cruz Biotech.

Zebrafish morphological and motor analysis

Zebrafish were characterized as described previously (Dowling et al., 2009; Dowling et al., 2010; Telfer et al., 2010). All images were obtained using a Nikon AZ100 macroscope or a Leica dissecting microscope.

Contractile properties

Zebrafish larvae were removed from 28°C and housed at room temperature for the testing period. Larvae were tested one at a time, alternating between experimental groups, because larvae were expected to develop over the ~6-hour period required for testing the given batch of larvae. The selected larva was anesthetized and tested in the following Tyrode's solution containing 0.02% tricaine (in mM): 136.5 NaCl, 5.0 KCl, 1.8 $CaCl_2$, 0.5 $MgCl_2$, 0.4 NaH_2PO_4, 11.9 $NaHCO_3$ and 0.1 EDTA (pH 7.3; maintained at 25°C). The larva was mounted horizontally into an experimental chamber designed for use with small muscle preparations (Claflin and Brooks, 2008), with one end attached to a stationary post and the other to a force transducer (400A, Aurora Scientific). Monofilament nylon suture (size 10-0) was used to fix the larva in place, with ties placed anterior to the swim bladder and near the posterior end of the larva. The experimental chamber was placed on an inverted microscope (Axiovert 100, Zeiss) and muscle striations were viewed through the transparent chamber bottom. A video system (900B, Aurora Scientific) monitored striation spacing and reported sarcomere length, which was adjusted by changing the length of the larva preparation. The sarcomere length was set to 2.1 μm to ensure maximal active twitch force (Dou et al., 2008). Activation of the preparation was accomplished by electrical field stimulation using a current stimulator (701C, Aurora Scientific), and the current intensity of 0.2 ms duration stimulus pulses was adjusted to elicit maximal active force. Once length and stimulation intensity were optimized, the larva was subjected to a single isometric contraction and force data were collected. After mechanical testing, the preparation remained at optimal length and the width of the trunk as viewed from ventral and lateral aspects of the preparation was measured near an anatomical landmark. CSA was estimated from these measurements assuming an ellipse. Peak force, CSA, normalized peak force, time-to-peak force and half-relaxation time, defined as the time required for peak twitch force to decay to 50%, were compared with unpaired *t*-tests.

Electron microscopy

Embryos and larvae were euthanized on ice and then fixed overnight in Karnovsky's fixative. Samples were then dehydrated and embedded in epon. Semi-thin sections were cut and stained with toluidine blue. Ultra-thin sections were cut on a microtome and then visualized with a Phillips transmission electron microscope. Sample preparation

RESOURCE IMPACT

Background

Nemaline myopathy (NM) is a severe and common childhood-onset muscle disease associated with significant disability and premature lethality. No cure or disease-modifying treatment currently exists for this devastating disorder. There are six gene mutations associated with NM, with mutations in *NEBULIN* (*NEB*) being most common. Mouse models involving *Neb* deficiency, dominant *ACTA1* mutations and dominant *TPM3* mutations recapitulate features of the human disease and have been instrumental for advancing knowledge about the pathogenesis of NM. However, they are not well suited for therapy development and, in particular, are not amenable to drug discovery studies using medium- or high-throughput techniques. Conversely, NM cannot be modeled in invertebrates because of significant dissimilarities in the fundament biology of the thin filament. Therefore, development of a zebrafish model of NM is important to bridge the need for improved genetic and chemical manipulation in a biologically relevant vertebrate organism.

Results

This paper characterizes the first zebrafish model of NM. These zebrafish, which were obtained from the Sanger Zebrafish Mutation Resource, carry a splice-site mutation in the *nebulin* gene that results in altered splicing and reduced levels of Nebulin protein. They have a dramatic phenotype, with significantly impaired motor function and greatly reduced survival. They also share all of the cardinal histopathological features of the human disease, including especially abnormal thin filament length, greatly reduced muscle force generation and the presence of nemaline bodies.

Implications and future directions

neb zebrafish provide an ideal model for therapy development for NM. In particular, they are well suited for testing gene-based therapies and for large-scale chemical screening to identify modifiers of the disease phenotype that can serve as putative therapeutic targets. *neb* zebrafish will also be useful for addressing key questions related to nebulin function and the pathogenesis of NM.

and imaging was performed by the Microscopy and Imaging Laboratory (MIL) at the University of Michigan.

Immunohistochemistry

Myofibers were prepared and isolated using a previously published technique (Dowling et al., 2009). In short, whole embryos were euthanized on ice and then dissociated in collagenase. Once dissociated, preps were filtered first through an 80 μm and then through a 40 μm filter (Falcon), resuspended in CO– independent media (Gibco), and then plated on coverslips coated with poly-L-ornithine. After approximately 1 hour, samples were fixed with 4% paraformaldehyde for 15 minutes and then processed for immunohistochemistry. Primary antibodies were to α-actinin (Sigma) and tropomodulin (Protein Tech Group). Alexa-Fluor-488 and -594-conjugated secondary antibodies were obtained from Invitrogen.

ACKNOWLEDGEMENTS

The authors thank Eva Feldman for thoughtful comments on the manuscript, Angela Busta for assistance with zebrafish husbandry, and Ann Davidson and Xingli Li for technical assistance.

COMPETING INTERESTS

The authors declare that they do not have any competing or financial interests.

AUTHOR CONTRIBUTIONS

J.J.D. conceived and designed the experiments and authored the manuscript. W.R.T. and T.W. participated in experimental design and performed the majority of the experiments. D.D.N. and S.V.B. conceived, designed and performed the contractile property measurements.

FUNDING

This work was funded in part by the Amendt-Heller Award from the Department of Pediatrics at the University of Michigan; by Foundation Building Strength; and by the National Institutes of Health [1K08AR054835 (to J.J.D.) and AG-020591 (to S.V.B.)].

SUPPLEMENTARY MATERIAL

Supplementary material for this article is available at http://dmm.biologists.org/lookup/suppl/doi:10.1242/dmm.008631/-/DC1

REFERENCES

Agrawal, P. B., Greenleaf, R. S., Tomczak, K. K., Lehtokari, V. L., Wallgren-Pettersson, C., Wallefeld, W., Laing, N. G., Darras, B. T., Maciver, S. K., Dormitzer, P. R. et al. (2007). Nemaline myopathy with minicores caused by mutation of the CFL2 gene encoding the skeletal muscle actin-binding protein, cofilin-2. *Am. J. Hum. Genet.* **80**, 162-167.

Bang, M. L., Li, X., Littlefield, R., Bremner, S., Thor, A., Knowlton, K. U., Lieber, R. L. and Chen, J. (2006). Nebulin-deficient mice exhibit shorter thin filament lengths and reduced contractile function in skeletal muscle. *J. Cell Biol.* **173**, 905-916.

Bassett, D. I. and Currie, P. D. (2003). The zebrafish as a model for muscular dystrophy and congenital myopathy. *Hum. Mol. Genet.* **12**, R265-R270.

Chandra, M., Mamidi, R., Ford, S., Hidalgo, C., Witt, C., Ottenheijm, C., Labeit, S. and Granzier, H. (2009). Nebulin alters cross-bridge cycling kinetics and increases thin filament activation: a novel mechanism for increasing tension and reducing tension cost. *J. Biol. Chem.* **284**, 30889-30896.

Claflin, D. R. and Brooks, S. V. (2008). Direct observation of failing fibers in muscles of dystrophic mice provides mechanistic insight into muscular dystrophy. *Am. J. Physiol. Cell Physiol.* **294**, C651-C658.

Darin, N. and Tulinius, M. (2000). Neuromuscular disorders in childhood: a descriptive epidemiological study from western Sweden. *Neuromuscul. Disord.* **10**, 1-9.

de Haan, A., van der Vliet, M. R., Gommans, I. M., Hardeman, E. C. and van Engelen, B. G. (2002). Skeletal muscle of mice with a mutation in slow alpha-tropomyosin is weaker at lower lengths. *Neuromuscul. Disord.* **12**, 952-957.

Donner, K., Ollikainen, M., Ridanpaa, M., Christen, H. J., Goebel, H. H., de Visser, M., Pelin, K. and Wallgren-Pettersson, C. (2002). Mutations in the beta-tropomyosin (TPM2) gene-a rare cause of nemaline myopathy. *Neuromuscul. Disord.* **12**, 151-158.

Donner, K., Sandbacka, M., Lehtokari, V. L., Wallgren-Pettersson, C. and Pelin, K. (2004). Complete genomic structure of the human nebulin gene and identification of alternatively spliced transcripts. *Eur. J. Hum. Genet.* **12**, 744-751.

Dou, Y., Andersson-Lendahl, M. and Arner, A. (2008). Structure and function of skeletal muscle in zebrafish early larvae. *J. Gen. Physiol.* **131**, 445-453.

Dowling, J. J., Vreede, A. P., Low, S. E., Gibbs, E. M., Kuwada, J. Y., Bonnemann, C. G. and Feldman, E. L. (2009). Loss of myotubularin function results in T-tubule disorganization in zebrafish and human myotubular myopathy. *PLoS Genet.* **5**, e1000372.

Dowling, J. J., Low, S. E., Busta, A. S. and Feldman, E. L. (2010). Zebrafish MTMR14 is required for excitation-contraction coupling, developmental motor function and the regulation of autophagy. *Hum. Mol. Genet.* **19**, 2668-2681.

Gokhin, D. S., Bang, M. L., Zhang, J., Chen, J. and Lieber, R. L. (2009). Reduced thin filament length in nebulin-knockout skeletal muscle alters isometric contractile properties. *Am. J. Physiol. Cell Physiol.* **296**, C1123-C1132.

Jin, J. P., Brotto, M. A., Hossain, M. M., Huang, Q. Q., Brotto, L. S., Nosek, T. M., Morton, D. H. and Crawford, T. O. (2003). Truncation by Glu180 nonsense mutation results in complete loss of slow skeletal muscle troponin T in a lethal nemaline myopathy. *J. Biol. Chem.* **278**, 26159-26165.

Jones, H. R., De Vivo, D. C. and Darras, B. T. (2003). *Neuromuscular Disorders of Infancy, Childhood, and Adolescence: a Clinician's Approach*. Amsterdam; Boston: Butterworth-Heinemann.

Labeit, S., Ottenheijm, C. A. and Granzier, H. (2011). Nebulin, a major player in muscle health and disease. *FASEB J.* **25**, 822-829.

Laing, N. G. and Wallgren-Pettersson, C. (2009). 161st ENMC International Workshop on nemaline myopathy and related disorders, Newcastle upon Tyne, 2008. *Neuromuscul. Disord.* **19**, 300-305.

Laing, N. G., Wilton, S. D., Akkari, P. A., Dorosz, S., Boundy, K., Kneebone, C., Blumbergs, P., White, S., Watkins, H., Love, D. R. et al. (1995). A mutation in the alpha tropomyosin gene TPM3 associated with autosomal dominant nemaline myopathy. *Nat. Genet.* **9**, 75-79.

Lehtokari, V. L., Plin, K., Sandbacka, M., Ranta, S., Donner, K., Muntoni, F., Sewry, C., Angelini, C., Bushby, K., Van den Bergh, P. et al. (2006). Identification of 45 novel mutations in the nebulin gene associated with autosomal recessive nemaline myopathy. *Hum. Mutat.* **27**, 946-956.

McElhinny, A. S., Schwach, C., Valichnac, M., Mount-Patrick, S. and Gregorio, C. C. (2005). Nebulin regulates the assembly and lengths of the thin filaments in striated muscle. *J. Cell Biol.* **170**, 947-957.

North, K. and Ryan, M. M. (1993). Nemaline myopathy. In *GeneReviews* (ed. R. A. Pagon, T. D. Bird, C. R. Dolan and K. Stephens). Seattle, WA: University of Washington.

Ochala, J. (2008). Thin filament proteins mutations associated with skeletal myopathies: defective regulation of muscle contraction. *J. Mol. Med. (Berl.)* **86**, 1197-1204.

Ochala, J., Lehtokari, V. L., Iwamoto, H., Li, M., Feng, H. Z., Jin, J. P., Yagi, N., Wallgren-Pettersson, C., Penisson-Besnier, I. and Larsson, L. (2011). Disrupted myosin cross-bridge cycling kinetics triggers muscle weakness in nebulin-related myopathy. *FASEB J*. **25**, 1903-1913.

Ottenheijm, C. A. and Granzier, H. (2010). Lifting the nebula: novel insights into skeletal muscle contractility. *Physiology (Bethesda)* **25**, 304-310.

Ottenheijm, C. A., Witt, C. C., Stienen, G. J., Labeit, S., Beggs, A. H. and Granzier, H. (2009). Thin filament length dysregulation contributes to muscle weakness in nemaline myopathy patients with nebulin deficiency. *Hum. Mol. Genet.* **18**, 2359-2369.

Ottenheijm, C. A., Lawlor, M. W., Stienen, G. J., Granzier, H. and Beggs, A. H. (2011). Changes in cross-bridge cycling underlie muscle weakness in patients with tropomyosin 3-based myopathy. *Hum. Mol. Genet*. **20**, 2015-2025.

Pappas, C. T., Krieg, P. A. and Gregorio, C. C. (2010). Nebulin regulates actin filament lengths by a stabilization mechanism. *J. Cell Biol.* **189**, 859-870.

Pappas, C. T., Bliss, K. T., Zieseniss, A. and Gregorio, C. C. (2011). The Nebulin family: an actin support group. *Trends Cell Biol*. **21**, 29-37.

Pelin, K., Hilpela, P., Donner, K., Sewry, C., Akkari, P. A., Wilton, S. D., Wattanasirichaigoon, D., Bang, M. L., Centner, T., Hanefeld, F. et al. (1999). Mutations in the nebulin gene associated with autosomal recessive nemaline myopathy. *Proc. Natl. Acad. Sci. USA* **96**, 2305-2310.

Ravenscroft, G., Jackaman, C., Bringans, S., Papadimitriou, J. M., Griffiths, L. M., McNamara, E., Bakker, A. J., Davies, K. E., Laing, N. G. and Nowak, K. J. (2011). Mouse models of dominant ACTA1 disease recapitulate human disease and provide insight into therapies. *Brain* **134**, 1101-1115.

Ryan, M. M., Schnell, C., Strickland, C. D., Shield, L. K., Morgan, G., Iannaccone, S. T., Laing, N. G., Beggs, A. H. and North, K. N. (2001). Nemaline myopathy: a clinical study of 143 cases. *Ann. Neurol.* **50**, 312-320.

Saint-Amant, L. and Drapeau, P. (1998). Time course of the development of motor behaviors in the zebrafish embryo. *J. Neurobiol.* **37**, 622-632.

Schroder, J. M., Durling, H. and Laing, N. (2004). Actin myopathy with nemaline bodies, intranuclear rods, and a heterozygous mutation in ACTA1 (Asp154Asn). *Acta Neuropathol.* **108**, 250-256.

Sparrow, J. C., Nowak, K. J., Durling, H. J., Beggs, A. H., Wallgren-Pettersson, C., Romero, N., Nonaka, I. and Laing, N. G. (2003). Muscle disease caused by mutations in the skeletal muscle alpha-actin gene (ACTA1). *Neuromuscul. Disord.* **13**, 519-531.

Telfer, W. R., Busta, A. S., Bonnemann, C. G., Feldman, E. L. and Dowling, J. J. (2010). Zebrafish models of collagen VI-related myopathies. *Hum. Mol. Genet.* **19**, 2433-2444.

Wallgren-Pettersson, C., Jasani, B., Newman, G. R., Morris, G. E., Jones, S., Singhrao, S., Clarke, A., Virtanen, I., Holmberg, C. and Rapola, J. (1995). Alpha-actinin in nemaline bodies in congenital nemaline myopathy: immunological confirmation by light and electron microscopy. *Neuromuscul. Disord.* **5**, 93-104.

Witt, C. C., Burkart, C., Labeit, D., McNabb, M., Wu, Y., Granzier, H. and Labeit, S. (2006). Nebulin regulates thin filament length, contractility, and Z-disk structure in vivo. *EMBO J.* **25**, 3843-3855.